Separation Science and Technology

ISSN: 0149-6395 (Print) 1520-5754 (Online) Journal homepage: http://www.tandfonline.com/loi/lsst20

APPLICATION OF EXTENDED KALMAN FILTER TO A BATCH COOLING CRYSTALLIZER

W. Xie & S. Rohani

To cite this article: W. Xie & S. Rohani (2001) APPLICATION OF EXTENDED KALMAN FILTER TO A BATCH COOLING CRYSTALLIZER, Separation Science and Technology, 36:13, 3049-3069, DOI: 10.1081/SS-100107645

To link to this article: http://dx.doi.org/10.1081/SS-100107645

Published online: 15 Feb 2007.

SEPARATION SCIENCE AND TECHNOLOGY, 36(13), 3049–3069 (2001)

APPLICATION OF EXTENDED KALMAN FILTER TO A BATCH COOLING CRYSTALLIZER

W. Xie and S. Rohani*

Department of Chemical and Biochemical Engineering,
University of Western Ontario, London,
Ontario N6A 5B9, Canada

ABSTRACT

The application of the extended Kalman filter (EKF) to a batch cooling crystallization process is presented. The simulation results point out that the feasibility of the on-line application of this nonlinear state estimation technique to a noisy nonlinear system heavily depends on the accurate measurement of the crystallizer temperature and the dissolved solute concentration. The EKF can reduce the effect of significant amounts of random noise in the measurements.

Key Words: Extended Kalman filter; Batch cooling crystallizer; Simulation study

*Corresponding author. E-mail: rohani@eng.uwo.ca

INTRODUCTION

The implementation of modern control theory requires knowledge of the state variable values in the system of interest. In many process situations, due to the lack of complete measurements of the states, state estimation problems are common.

In 1960, Kalman (1) first developed an optimal, sequential, discrete-time estimation technique. A year later, Kalman and Bucy derived maximum likelihood estimates of measured and unmeasured process states (2). This approach combined the information from a mathematical model of the process with actual process measurements. Since then, many theoretical and applied extensions of state identification have been presented. The extended Kalman filter (EKF), as an approximate filter for nonlinear systems, was applied by Gavalas and Seinfeld (3) to tubular reactors, by Seinfeld (4) to a continuous stirred tank reactor (CSTR) with a first-order exothermic reaction, by Wells (5) to a 6-dimension nonlinear well-stirred reactor, and by Wismer and Wells (6) to the basic oxygen furnace. Coggan and Wilson (7) demonstrated the applications of the Kalman sequential estimator to industrial processes for on-line state estimation. In Hamilton, Seborg, and Fisher (8), simulation and experimental studies were carried out for the comparison of the Kalman filter with an exponential filter. In 1986, Jang, Joseph, and Muka (9) compared the EKF approach with the horizon approach to the on-line parameter and state estimation of the nonlinear systems of Seinfeld (4). Simultaneous state and parameter identification was successfully presented by Stephanopoulos and San (10) and San and Stephanopoulos (11) in a biochemical reactor. Ramirez (12) showed the advantages of coupling a sequential parameter identification algorithm with the Kalman filter state identification algorithm in a batch fermentation process. The EKF as a state estimator was employed by Dimitratos et al. (13) for an emulsion copolymerization reactor and by Kozub and Macgregor (14) for semi-batch polymerization reactors. Myers and Luecke (15) described an efficient new algorithm of the EKF. This new algorithm exploited the decoupled nature of the state estimate and error covariance equations along with the symmetry of the error covariance matrix. Lee and Ricker (16) illustrated the EKF-based nonlinear-model predictive control technique using successive linearization. Recently, Ahn, Park, and Rhee (17) successfully applied the EKF-based nonlinear-model predictive control for a continuous methyl methacrylate (MMA) polymerization reactor. Jazwinski (18) and Gelb (19) present 2 good books that discuss the theory of filtering and the applications of optimal estimation in detail.

The objective of this study was to find a useful way to overcome the major obstacles of the lack of direct on-line measurements in the batch cooling crystallization process and make the implementation of the advanced-model based control strategies possible.

In this study, the standard algorithm of the EKF is presented. The possibility of EKF application as a nonlinear estimator of the batch cooling crystallization process is discussed. We found that crystallizer temperature and dissolved solute

MARCEL DEKKER, INC.
270 Madison Avenue, New York, New York 10016

concentration are critical measurements that determine the feasibility of EKF application to a batch cooling crystallizer.

ALGORITHM OF THE EKF

The EKF is a recursive state estimator providing minimum-variance state estimation. To develop the EKF, one should formulate a dynamic model of the system as a set of ordinary differential equations with the observation equations:

$$\begin{aligned} \dot{x} &= f\,(x,t) + w \\ Z_k &= h(x_k) + v_k \end{aligned} \tag{1}$$

where, x is the state variable; Z_k is the measured output; w is the process error; and v_k describes the measurement error. Both are uncorrelated zero-mean Gaussian noise processes with covariance matrix Q and R_k, respectively. Because the process is continuous and the system outputs are discrete, as measured at sampling times, the model is defined in the continuous-discrete form.

The EKF is comprised of 2 recursive update stages: the model-based update stage and the measurement-based update stage.

Model-Based Update Stage

Based on the model, the estimates of the new states are updated over the time interval from $k - 1$ to k in the absence of new measurements. In this stage, the predictions of $\hat{x}_k(-)$ and $P(-)$, used in the measurement-based update stage, are calculated.

$$\begin{aligned} \dot{x}(t) &= f(\hat{x},t) \\ \hat{x}(0) &= x_0 \end{aligned} \tag{2}$$

$$\begin{aligned} \dot{P}(t) &= F(\hat{x},t)\,P(t) + P(t)\,F^{\mathrm{T}}\,(\hat{x},t) + Q(t) \\ P(0) &= P_0 \end{aligned} \tag{3}$$

where, $\dot{P}$ is the derivative of the state error covariance matrix; x_0 is the initial state with the error covariance P_0; F is the Jacobian matrix of f defined by

$$F(\hat{x},t) = \left(\frac{\partial f}{\partial x}\right)_{x=\hat{x}} \tag{4}$$

Measurement-Based Update Stage

Once the new measurements become available, corrections to the estimations $\hat{x}_k(-)$ and $P_i(-)$ are made by minimizing the estimation error. These corrected estimations are represented by $\hat{x}_k(+)$ and $P_i(+)$, respectively.

$$\hat{x}_k(+) = \hat{x}(-) + K_k \{Z_k - h [\hat{x}(-)]\} \tag{5}$$

$$P_k(+) = \{I - K_k H_k [\hat{x}_k (-)]\} P_k(-) \tag{6}$$

where, H_k is the Jacobian matrix of h

$$H_k [\hat{x}_k(-)] = \left(\frac{\partial h}{\partial x}\right)_{x=\hat{x}(-)} \tag{7}$$

and K_k is the Kalman gain matrix

$$K_k = P_k(-) H_k^T [\hat{x}_k(-)]\{H_k [\hat{x}_k(-)] P_k(-) H_k^T [\hat{x}_k(-)] + R_k\}^{-1} \tag{8}$$

At each integration step, solution of the EKF equations starts with integration of the model-based state estimate (Eq. 2) and the model-based state-error covariance (Eq. 4) through the use of the fourth-order Runge-Kutta method. Based on the new available measurements, corrections of the new predictions are then calculated through Eqs. (5) and (6).

SIMULATION STUDIES AND DISCUSSION

The EKF was used as an on-line nonlinear estimator to both provide estimates for the unmeasured states and to reduce the effect of measurement noise in the batch cooling crystallization process. The development of the dynamic model for the batch cooling crystallizer model is discussed in detail by Xie, Rohani, and Phoenix (20). The state space form of the model is given by

$$\dot{x} = f(x) \tag{9}$$

where

$$x^{\mathrm{T}} = [x_1 \cdots x_8] = [T_c \quad T_j \quad C \quad m_{\mathrm{N},0} \quad m_{\mathrm{N},1} \quad m_{\mathrm{N},2} \quad m_{\mathrm{N},3} \quad L_{\mathrm{s}}]$$

$$f(x) = \begin{bmatrix} f_1(x) \\ f_2(x) \\ f_3(x) \\ f_4(x) \\ f_5(x) \\ f_6(x) \\ f_7(x) \\ f_8(x) \end{bmatrix} = \begin{bmatrix} \dfrac{-UA(x_1 - x_2) - 3W\Delta H \rho_{\mathrm{c}} k_{\mathrm{v}} G(N_{\mathrm{s}} x_8^2 + x_6)}{W c_{p\mathrm{w}} (1 + x_3) + W \rho_{\mathrm{c}} k_{\mathrm{v}} c_{p\mathrm{c}} (N_{\mathrm{s}} x_8^3 + x_7)} \\ \dfrac{F_{\mathrm{w}}}{V_{\mathrm{j}}} (T_{\mathrm{j,in}} - x_2) + \dfrac{UA}{\rho_{\mathrm{w}} V_{\mathrm{j}} c_{p\mathrm{w}}} (x_1 - x_2) \\ -3\rho_{\mathrm{c}} k_{\mathrm{v}} G(N_{\mathrm{s}} x_8^2 + x_6) \\ B \\ x_4 G \\ 2x_5 G \\ 3x_6 G \\ G \end{bmatrix}$$

Table 1. The Operating Conditions and the Physical Properties of the Potash-Alum-Water System.

Initial Saturation Temperature	45°C	ρ_c	1760 kg/m^3 crystal
Initial temperature	40°C	k_v	1
Stirrer speed	13.2 rps	$U^{\cdot}A$	800 J/°C·s
W_s	10 g	ΔH	44.5 kJ/kg crystal(23)
ΔL_s	10 μm	$c_{p,c}$	0.84 kJ/°C·kg crystal
L_{s0}	150 μm	$c_{p,s}$	3.8 kJ/°C·kg solution
Crystallizer volume	27 L	Batch time	4600 seconds

$G(t) = k_g R^{2.76} \Delta C^{0.765}$ m/s, where $\Delta C = C - C^*$, $k_g = 1.25 \times 10^{-9}$
$B(t) = k_b M_T G^{1.88}$ no./ kg solvent·s; $k_b = 5.0 \times 10^{18}$

$C^* = a_0 + a_1[T_c\ (t) - 273.15] + a_2\ [T_c\ (t) - 273.15]^2$ kg solute/ kg solvent (24); $a_0 = 6.063 \times 10^{-2}$, $a_1 = 9.584 \times 10^{-4}$, $a_2 = 5.85 \times 10^{-5}$.

where the subscript T represents the transpose of a matrix; T_c is the crystallizer temperature; T_j is the inside cooling jacket temperature; $T_{j,in}$ is the inlet cooling jacket temperature; C is the dissolved solute concentration; $m_{N,0}$, $m_{N,1}$, $m_{N,2}$, and $m_{N,3}$ are the first 4 leading moments of the newly generated crystals; L_s is the size of the seed crystals; and B and G are the nucleation and growth kinetics of the crystallization as deduced by Tavare and Garside (21). Table 1 gives the physical and kinetic parameters of the potash-alum-water system used in the simulation study.

The normalized model of the batch cooling crystallizer is derived by substituting the normalized state variables into the original model of Eq. (9).

$$Z_1 = T_c / T_{c,max} \qquad Z_2 = T_j / T_{j,max} \qquad Z_3 = C / C_{max}$$
$$Z_4 = m_{0,N} / m_{0,N,max} \qquad Z_5 = m_{1,N} / m_{1,N,max}$$
$$Z_6 = m_{2,N} / m_{2,N,max} \qquad Z_7 = m_{3,N} / m_{3,N,max} \qquad Z_8 = L_s / L_{s,max} \qquad \theta = t/t_f$$

The resulting equation is

$$\dot{Z} = f(Z) \tag{10}$$

where

$$f_1 = \frac{-UA(T_{c,max} Z_1 - T_{j,max} Z_2) - 3W\Delta H \rho_c k_v G \times [N_s (L_{s,max} Z_8)^2 + m_{2,N,max} Z_6]}{Wc_{pw}(1 + C_{max} Z_3) + W\rho_c k_v c_{pc} \times [N_s (L_{s,max} Z_8)^3 + m_{3,N,max} Z_7]} \times \frac{tf}{T_{c,max}}$$

$$f_2 = \left[\frac{F_w}{V_j}(T_{j,in} - T_{j,max} Z_2) + \frac{UA}{\rho_w V_j c_{pw}}(T_{c,max} Z_1 - T_{j,max} Z_2)\right] \times \frac{t_f}{T_{j,max}}$$

$$f_3 = \{-3\rho_c k_v G [N_s (L_{s,max} Z_8)^2 + m_{2,N,max} Z_6]\} \times \frac{t_f}{C_{max}}$$

$$f_4 = B \times \frac{t_f}{m_{0,\mathrm{N,max}}}$$

$$f_5 = m_{0,\mathrm{N,max}}\, Z_4 G \times \frac{t_f}{m_{1,\mathrm{N,max}}}$$

$$f_6 = 2m_{1,\mathrm{N,max}}\, Z_5 G \times \frac{t_f}{m_{2,\mathrm{N,max}}}$$

$$f_7 = 3m_{2,\mathrm{N,max}}\, Z_5 G \times \frac{t_f}{m_{3,\mathrm{N,max}}}$$

$$f_8 = G \times \frac{t_f}{L_{\mathrm{s,max}}}$$

And the measured output is defined by

$$y_k = h_k(Z) + v_k = \begin{bmatrix} Z_{1k} \\ Z_{2k} \\ Z_{3k} \end{bmatrix} + v_k \tag{11}$$

The Jacobian matrix of F and H may be obtained by computing the partial derivatives with respect to each normalized state variables (see the Appendix).

$$F(t, \hat{Z}(t)) = \begin{bmatrix} \frac{\partial f_1}{\partial x_1} \cdots \frac{\partial f_1}{\partial x_8} \\ \vdots \quad\quad \vdots \\ \frac{\partial f_8}{\partial x_1} \cdots \frac{\partial f_8}{\partial x_8} \end{bmatrix}_{Z=\hat{Z}(t)} \tag{12}$$

$$H(t,\hat{Z}(t)) = \begin{bmatrix} 0 & 0 & 0 \\ 0 & 1 & 0 \\ 0 & 0 & 1 \end{bmatrix}_{Z=\hat{Z}(t)} \tag{13}$$

In the following section, we discuss the strategy of selecting measured variables and their influence on the performance of the EKF in a potash-alum batch cooling crystallizer. All measurements used are assumed to be sampled at an interval of 1 second and to be corrupted with Gaussian noise with a zero mean. Xie et al. (20) considered the performance of the EKF in the presence of mismatch (nucleation and growth kinetics constants) between the process model and the plant.

First, crystallizer temperature is chosen as the only measured variable because it can be measured conventionally and on-line. Based on the measurement of crystallizer temperature, other important state variables are estimated by the EKF.

Figures 1–7 show the tracking of each estimated state. Figure 1 shows that the EKF gives a very good prediction for the inside cooling-jacket temperature.

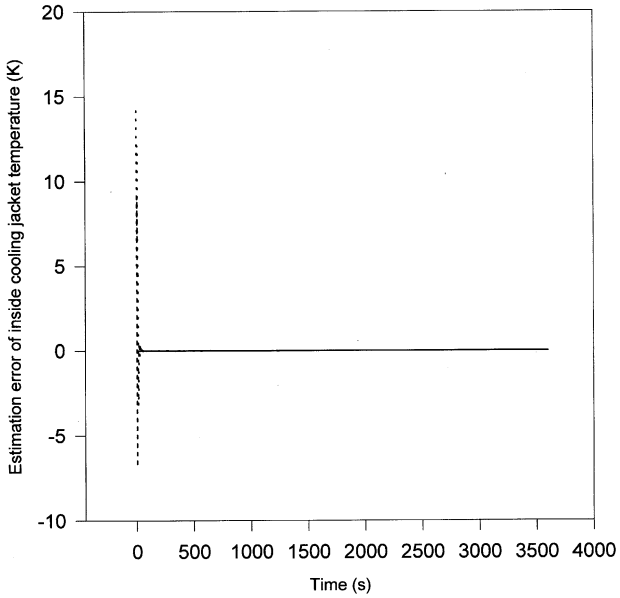

Figure 1. Inside cooling-jacket temperature and its estimation based on the measurement of crystallizer temperature.

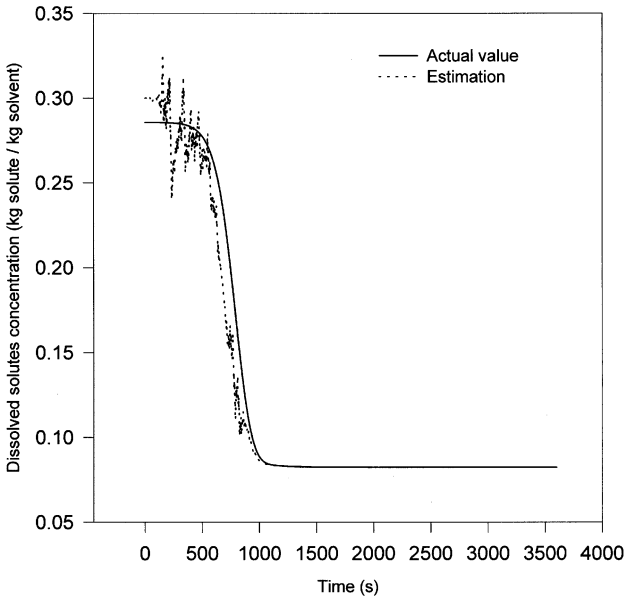

Figure 2. Dissolved solute concentration and its estimation based on the measurement of crystallizer temperature.

MARCEL DEKKER, INC.
270 Madison Avenue, New York, New York 10016

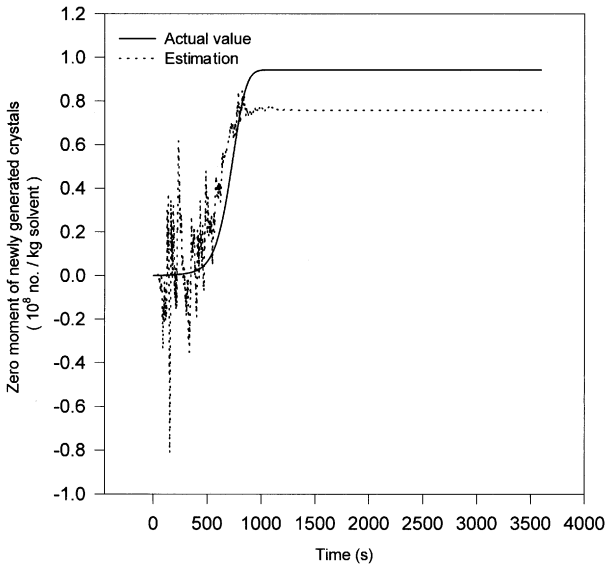

Figure 3. Zero moment of the newly generated crystals and its estimation based on the measurement of crystallizer temperature.

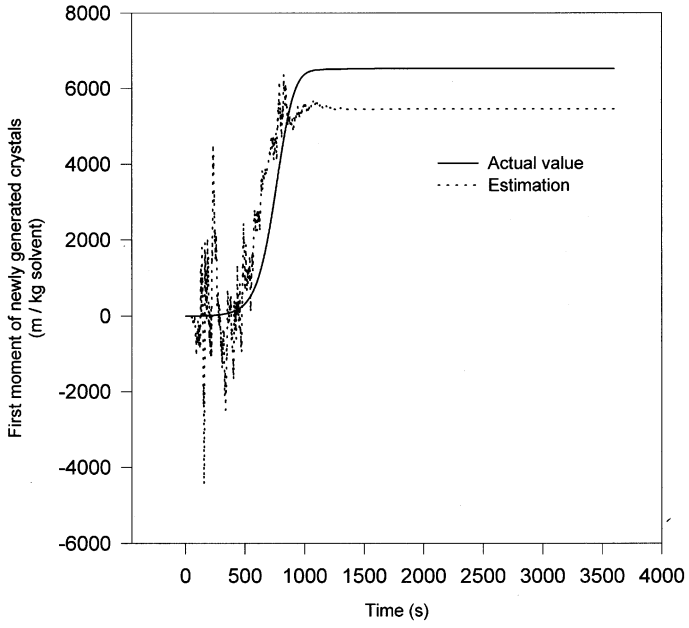

Figure 4. First moment of the newly generated crystals and its estimation based on the measurement of crystallizer temperature.

MARCEL DEKKER, INC.
270 Madison Avenue, New York, New York 10016

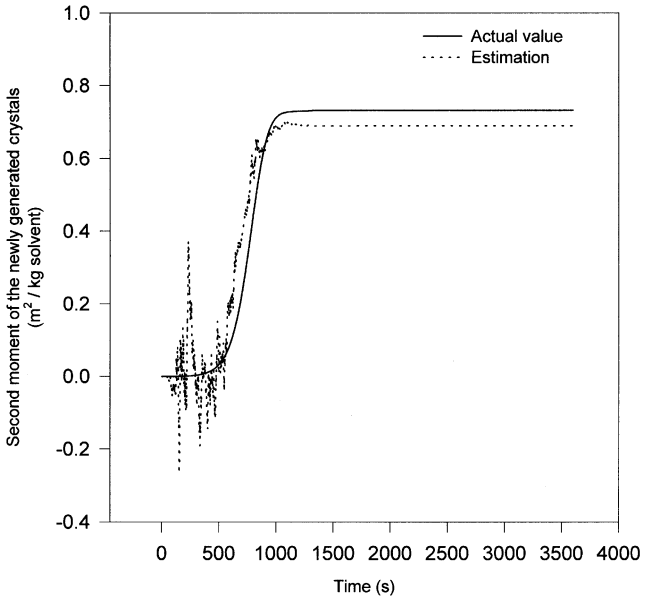

Figure 5. Second moment of the newly generated crystals and its estimation based on the measurement of crystallizer temperature.

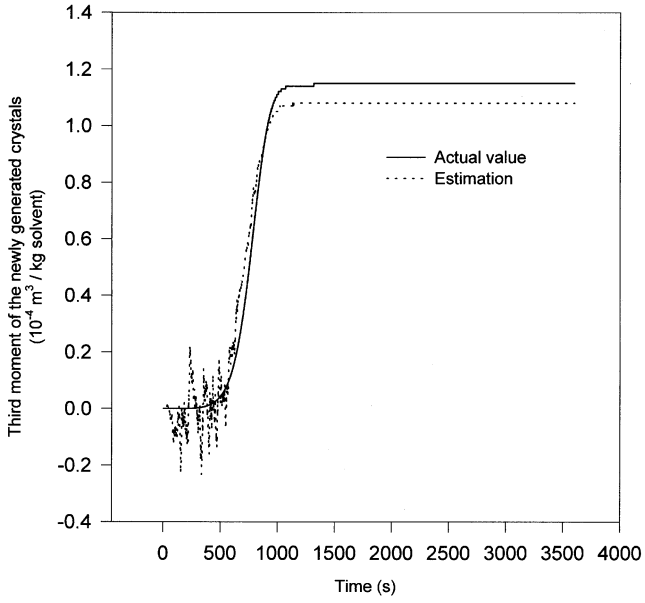

Figure 6. Third moment of the newly generated crystals and its estimation based on the measurement of crystallizer temperature.

MARCEL DEKKER, INC.
270 Madison Avenue, New York, New York 10016

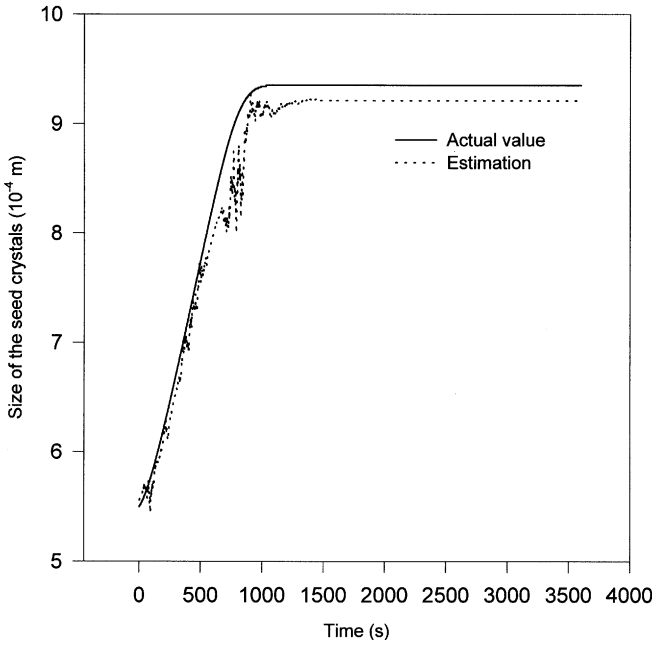

Figure 7. Size of the seed crystals and its estimation based on the measurement of crystallizer temperature.

The results are derived from the direct relationship between crystallizer temperature (the measurement) and inside cooling-jacket temperature (see f_2 in Eq. 9). Figure 2 demonstrates that the estimation of dissolved solute concentration can follow its actual value without offset at the end of the batch time. In batch cooling crystallization, supersaturation is represented by the difference between dissolved solute concentration and equilibrium concentration. Supersaturation is generated by reducing the solubility of the dissolved solute with a decrease of crystallizer temperature. The solubility equation [$C^*(T_c)$] in Table 1 gives a one-to-one relationship between crystallizer temperature and equilibrium concentration. So, an indirect but strong relationship exists between dissolved solute concentration and crystallizer temperature, which results in good convergence. The other states, such as the first 4 leading moments of the newly generated crystals and size of the seed crystals, have weak relationships with the crystallizer temperature. Moreover, the implementation of the EKF requires the linearization (by first-order Taylor series expansion) of the model at current estimated states, which eliminates some important information. Therefore, the predictions of these states are not very good. Figures 3–7 show that the predictions contain oscillations at the beginning and offset at the end.

MARCEL DEKKER, INC.
270 Madison Avenue, New York, New York 10016

New measurements should be introduced to the EKF to improve the accuracy of the predictions. One possible way to add new measurements is to set another thermocouple to measure inside cooling-jacket temperature. However, because the inside cooling-jacket temperature is only directly related to crystallizer temperature and the crystallizer temperature is already 1 of our measurements, this approach cannot improve the estimations of the state variables other than crystallizer temperature. The dissolved solute concentration is another variable that can be easily measured by an on-line density meter (22) or a refractive index sensor. Figures 8–11 demonstrate that introducing dissolved solute concentration as 1 measured variable improves significantly the performance of the EKF for the estimations of the first 4 leading moments of the newly generated crystals. After the initial period of oscillation, when the relative error in measurements is large, the true and estimated states are indistinguishable. First, measuring the dissolved solute concentration guarantees good prediction for itself through EKF by means of compensating for the measurement noise and uncertainty in the process. Second, better prediction of the third moment is based on good prediction of dissolved

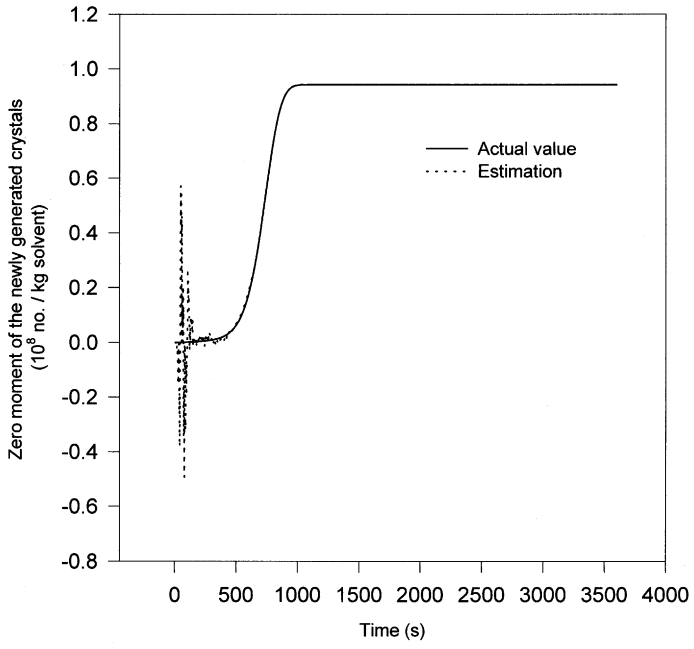

Figure 8. Zero moment of the newly generated crystals and its estimation based on the measurement of crystallizer temperature, inside cooling jacket temperature and dissolved solute concentration.

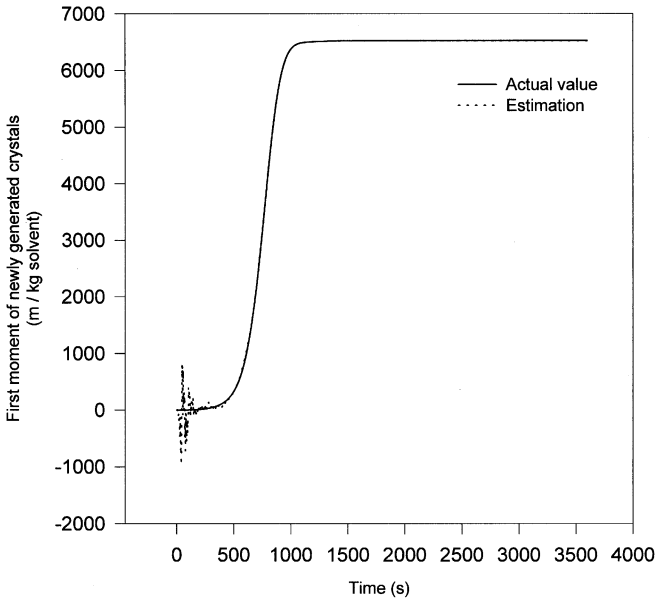

Figure 9. First moment of the newly generated crystals and its estimation based on the measurement of crystallizer temperature, inside cooling jacket temperature, and dissolved solute concentration.

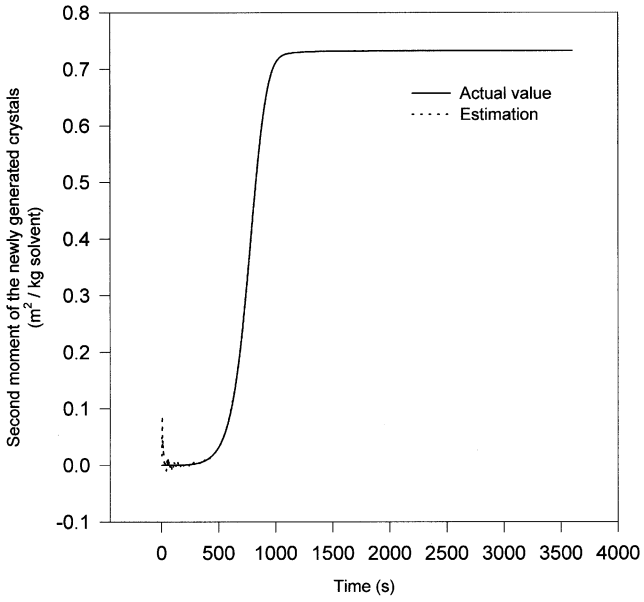

Figure 10. Second moment of the newly generated crystals and its estimation based on the measurement of crystallizer temperature, inside cooling jacket temperature, and dissolved solute concentration.

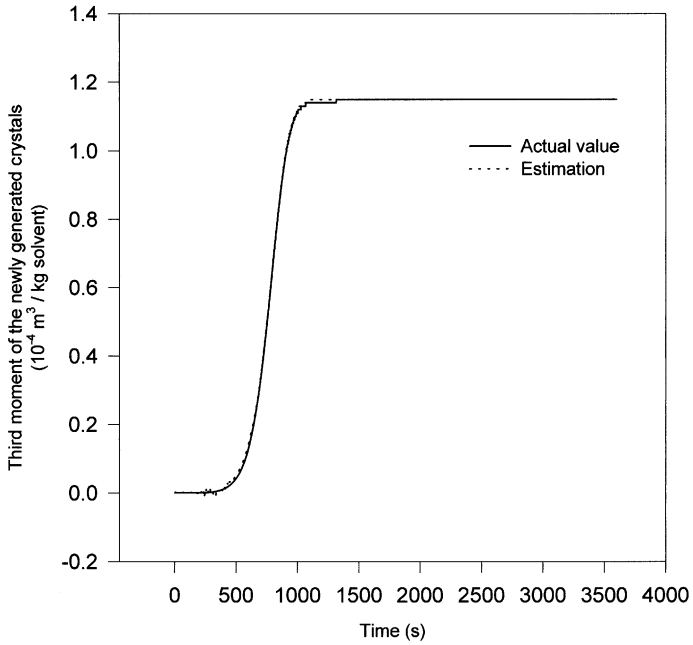

Figure 11. Third moment of the newly generated crystals and its estimation based on the measurement of crystallizer temperature, inside cooling jacket temperature, and dissolved solute concentration.

solute concentration (see f_3 in Eq. 9). Third, good estimation of the third moment guarantees the accurate prediction of other moments possible by the intrinsic link between moments.

In both systems discussed above, the effect on predictions of an addition of 10% Gaussian noise to the measurements, due to the good filtering capability of the EKF, was reduced significantly.

CONCLUSIONS

In this study, the EKF as a nonlinear estimator for a batch cooling crystallization system was investigated. The feasibility of application of the EKF in the batch cooling crystallization process heavily relied on the accurate on-line measurement of crystallizer temperature and dissolved solute concentration. Slow convergence from poor initial state estimates was found, which mainly resulted from the recursive nature of the algorithm. The EKF could compensate for the influence of the Gaussian noise in the measurement. Good prediction of the unmea-

sured variables provided by the EKF could facilitate the implementation of modern control theory in noisy nonlinear systems such as a batch cooling crystallization process.

APPENDIX: THE JACOBIAN MATRIX

$$F(t, \hat{Z}(t)) = \begin{bmatrix} \frac{\partial f_1}{\partial x_1} \cdots \frac{\partial f_1}{\partial x_8} \\ \vdots \quad\quad \vdots \\ \frac{\partial f_8}{\partial x_1} \cdots \frac{\partial f_8}{\partial x_8} \end{bmatrix}_{Z=\hat{Z}(t)}$$

where

$$\begin{aligned}
\partial f_1/\partial Z_1 = {} & \{-UA \times T_{c,max} - 2.295W\Delta H\rho_c k_v k_g R^{2.67}[N_s(L_{s,max}Z_8)^2 \\
& + m_{2,N,max}Z_6] \times \{-[a_1 T_{c,max} + 2a_2(T_{c,max}Z_1 \\
& - 273.15)T_{c,max}] / [1 - a_0 - a_1(T_{c,max}Z_1 - 273.15) \\
& - a_2(T_{c,max}Z_1 - 273.15)^2] + [a_0 + a_1(T_{c,max}Z_1 - 273.15) \\
& + a_2(T_{c,max}Z_1 - 273.15)^2] \\
& \times [-a_1 T_{c,max} - 2a_2(T_{c,max}Z_1 - 273.15)T_{c,max}] / \{[1 - a_0 \\
& - a_1(T_{c,max}Z_1 - 273.15) - a_2(T_{c,max}Z_1 - 273.15)^2]^2\}\} / \\
& \{\{Z_3 C_{max} - [a_0 + a_1(T_{c,max}Z_1 - 273.15) + a_2(T_{c,max}Z_1 \\
& - 273.15)^2]\} / [1 - a_0 - a_1(T_{c,max}Z_1 - 273.15) \\
& - a_2(T_{c,max}Z_1 - 273.15)^2]^{0.235}\}\} tf / \{\{Wc_{pw}(1 + Z_3 C_{max}) \\
& + W\rho_c k_v c_{pc}[N_s(L_{s,max}Z_8)^3 + m_{3,N,max}Z_7])\}T_{c,max}\}; \\
\partial f_1/\partial Z_2 = {} & UA \times T_{j,max} t_f / \{\{Wc_{pw}(1 + Z_3 C_{max}) + W\rho_c k_v c_{pc}[N_s(L_{s,max}Z_8)^3 \\
& + m_{3,N,max}Z_7]\}T_{c,max}\} \\
\partial f_1/\partial Z_3 = {} & -2.295W\Delta H\rho_c k_v k_g R^{2.67}[N_s(L_{s,max}Z_8)^2 + m_{2,N,max}Z_6]C_{max}t_f \\
& /\{\{Z_3 C_{max} - [a_0 + a_1(T_{c,max}Z_1 - 273.15) + a_2(T_{c,max}Z_1 \\
& - 273.15)^2] / [1 - a_0 - a_1(T_{c,max}Z_1 - 273.15) \\
& - a_2(T_{c,max}Z_1 - 273.15)^2]\}^{0.235}\{Wc_{pw}(1 + Z_3 C_{max}) \\
& + W\rho_c k_v c_{pc}[N_s(L_{s,max}Z_8)^3 + m_{3,N,max}Z_7]\}T_{c,max} - \{-UA \\
& \times (T_{c,max}Z_1 - T_{j,max}Z_2) - 3W\Delta H\rho_c k_v k_g R^{2.67}\{Z_3 C_{max} - \\
& [a_0 + a_1(T_{c,max}Z_1 - 273.15) + a_2(T_{c,max}Z_1 - 273.15)^2] / [1 \\
& - a_0 - a_1(T_{c,max}Z_1 - 273.15) - a_2(T_{c,max}Z_1 - 273.15)^2] / \\
& [1 - a_0 - a_1(T_{c,max}Z_1 - 273.15) - a_2(T_{c,max}Z_1 - \\
& 273.15)^2]\}^{0.765} \times [N_s(L_{s,max}Z_8)^2 + m_{2,N,max}Z_6]\}t_f \times \\
& Wc_{pw}C_{max} /\{\{Wc_{pw}(1 + Z_3 C_{max}) + W\rho_c k_v c_{pc}[N_s(L_{s,max}Z_8)^3 \\
& + m_{3,N,max}Z_7]\}^2 T_{c,max}\}; \\
\partial f_1/\partial Z_4 = {} & 0; \partial f_1/\partial Z_5 = 0; \\
\partial f_1/\partial Z_6 = {} & -3W\Delta H\rho_c k_v k_g R^{2.67}\{Z_3 C_{max} - [a_0 + a_1(T_{c,max}Z_1 - 273.15) \\
& + a_2(T_{c,max}Z_1 - 273.15)^2] / [1 - a_0 - a_1(T_{c,max}Z_1 - 273.15)
\end{aligned}$$

$$
\begin{aligned}
&- a_2(T_{\mathrm{c,max}}Z_1 - 273.15)^2]\}^{0.765}\, m_{2,N,\mathrm{max}}\, t_f / \{Wc_{pw}(1 \\
&+ Z_3C_{\mathrm{max}}) + W\rho_c k_v c_{pc}[N_s(L_{s,\mathrm{max}}Z_8)^3 + m_{3,\mathrm{N,max}}Z_7)]^2 T_{\mathrm{c,max}}\}; \\
\partial f_1/\partial Z_7 = &-\{- UA \times (T_{\mathrm{c,max}}Z_1 - T_{\mathrm{j,max}}Z_2) - 3W\Delta H\rho_c k_v k_g \\
&R^{2.67}(Z_3C_{\mathrm{max}} - [a_0 + a_1(T_{\mathrm{c,max}}Z_1 - 273.15) + a_2(T_{\mathrm{c,max}}Z_1 \\
&- 273.15)^2]/[1 - a_0 - a_1(T_{\mathrm{c,max}}Z_1 - 273.15) - a_2(T_{\mathrm{c,max}}Z_1 \\
&- 273.15)^2]\}^{0.765}\, [N_s(L_{s,\mathrm{max}}Z_8)^2 + m_{2,\mathrm{N,max}}Z_6)]t_f \\
&\times W\rho_c k_v c_{pc} m_{3,\mathrm{N,max}} / \{\{Wc_{\mathrm{pw}}(1 + Z_3C_{\mathrm{max}}) \\
&+ W\rho_c k_v c_{pc}[N_s(L_{s,\mathrm{max}}Z_8)^3 + m_{3,\mathrm{N,max}}Z_7]\}^2 T_{\mathrm{c,max}}\}; \\
\partial f_1/\partial Z_8 = &-6W\Delta H\rho_c k_v k_g\, R^{2.67}\{Z_3C_{\mathrm{max}} - [a_0 + a_1(T_{\mathrm{c,max}}Z_1 - 273.15) \\
&+ a_2(T_{\mathrm{c,max}}Z_1 - 273.15)^2] / [1 - a_0 - a_1(T_{\mathrm{c,max}}Z_1 - 273.15) \\
&- a_2(T_{\mathrm{c,max}}Z_1 - 273.15)^2]\}^{0.765}\, N_s L_{s,\mathrm{max}}{}^2 Z_8 t_f / \{\{Wc_{pw}(1 \\
&+ Z_3C_{\mathrm{max}}) + W\rho_c k_v c_{pc}[N_s(L_{s,\mathrm{max}}Z_8)^3 + m_{3,\mathrm{N,max}}Z_7]\}^2 T_{\mathrm{c,max}}\} \\
&- 3[- UA \times (T_{\mathrm{c,max}}Z_1 - T_{\mathrm{j,max}}Z_2) - 3W\Delta H\rho_c k_v k_g \\
&R^{2.67}\{Z_3C_{\mathrm{max}} - [a_0 + a_1(T_{\mathrm{c,max}}Z_1 - 273.15) + a_2(T_{\mathrm{c,max}}Z_1 \\
&- 273.15)^2] / [1 - a_0 - a_1(T_{\mathrm{c,max}}Z_1 - 273.15) - a_2(T_{c,\mathrm{max}}Z_1 \\
&- 273.15)^2]\}^{0.765}\, [N_s(L_{s,\mathrm{max}}Z_8)^2 + m_{2,\mathrm{N,max}}Z_6)]t_f \times \\
&W\rho_c k_v c_{pc} N_s L_{s,\mathrm{max}}{}^3 Z_8{}^2 / \{\{Wc_{pw}(1 + Z_3C_{\mathrm{max}}) + W\rho_c k_v c_{pc} \\
&\times [N_s(L_{s,\mathrm{max}}Z_8)^3 + m_{3,\mathrm{N,max}}Z_7]\}^2 T_{\mathrm{c,max}}\} \\
\partial f_2/\partial Z_1 = &\; UA \times T_{\mathrm{c,max}}\, t_f / (\rho_c V_j c_{pw} T_{\mathrm{j,max}}); \\
\partial f_2/\partial Z_2 = &- T_{\mathrm{j,max}} F_w / V_j - UA \times t_f / (\rho\, V_j c_{pw}); \\
\partial f_2/\partial Z_3 = &\; 0;\ \partial f_2/\partial Z_4 = 0;\ \partial f_2/\partial Z_5 = 0;\ \partial f_2/\partial Z_6 = 0;\ \partial f_2/\partial Z_7 = 0; \\
&\partial f_2/\partial Z_8 = 0 \\
\partial f_3/\partial Z_1 = &- 2.295\rho_c k_v k_g R^{2.67}[N_s(L_{s,\mathrm{max}}Z_8)^2 + m_{2,\mathrm{N,max}}Z_6]t_f \times \\
&\{-[a_1 T_{\mathrm{c,max}} + 2a_2(T_{\mathrm{c,max}}Z_1 - 273.15)T_{\mathrm{c,max}}] / [1 - a_0 \\
&- a_1(T_{\mathrm{c,max}}Z_1 - 273.15) - a_2(T_{\mathrm{c,max}}Z_1 - 273.15)^2] + [a_0 \\
&+ a_1(T_{\mathrm{c,max}}Z_1 - 273.15) + a_2(T_{\mathrm{c,max}}Z_1 - 273.15)^2] \\
&\times [-a_1 T_{\mathrm{c,max}} - 2a_2(T_{\mathrm{c,max}}Z_1 - 273.15)T_{\mathrm{c,max}}] / \{[1 - a_0 \\
&- a_1(T_{\mathrm{c,max}}Z_1 - 273.15) - a_2(T_{\mathrm{c,max}}Z_1 - 273.15)^2]^2\}\} / \\
&\{\{Z_3C_{\mathrm{max}} - [a_0 + a_1(T_{\mathrm{c,max}}Z_1 - 273.15) + a_2(T_{\mathrm{c,max}}Z_1 \\
&- 273.15)^2] / [1 - a_0 - a_1(T_{\mathrm{c,max}}Z_1 - 273.15) - a_2(T_{\mathrm{c,max}}Z_1 \\
&- 273.15)^2]\}^{0.235} C_{\mathrm{max}}\} \\
\partial f_3/\partial Z_2 = &\; 0; \\
\partial f_3/\partial Z_3 = &- 2.295\rho_c k_v k_g R^{2.67}[N_s(L_{s,\mathrm{max}}Z_8)^2 + m_{2,\mathrm{N,max}}Z_6]t_f / \{\{Z_3C_{\mathrm{max}} \\
&- [a_0 + a_1(T_{\mathrm{c,max}}Z_1 - 273.15) + a_2(T_{\mathrm{c,max}}Z_1 - 273.15)^2] / \\
&[1 - a_0 - a_1(T_{\mathrm{c,max}}Z_1 - 273.15) - a_2(T_{\mathrm{c,max}}Z_1 \\
&- 273.15)^2]\}^{0.235}\} \\
\partial f_3/\partial Z_4 = &\; 0;\ \partial f_3/\partial Z_5 = 0; \\
\partial f_3/\partial Z_6 = &- 3\rho_c k_v k_g R^{2.67}\{Z_3C_{\mathrm{max}} - [a_0 + a_1(T_{\mathrm{c,max}}Z_1 - 273.15) \\
&+ a_2(T_{\mathrm{c,max}}Z_1 - 273.15)^2\,] / [1 - a_0 - a_1(T_{\mathrm{c,max}}Z_1 \\
&- 273.15) - a_2(T_{\mathrm{c,max}}Z_1 - 273.15)^2]\}^{0.765} m_{2,\mathrm{N,max}}\, t_f / C_{\mathrm{max}} \\
\partial f_3/\partial Z_7 = &\; 0;
\end{aligned}
$$

$$\partial f_3/\partial Z_8 = -6\rho_c k_v k_g R^{2.67}\{Z_3 C_{max} - [a_0 + a_1(T_{c,max}Z_1 - 273.15) + a_2(T_{c,max}Z_1 - 273.15)^2]/[1 - a_0 - a_1(T_{c,max}Z_1 - 273.15) - a_2(T_{c,max}Z_1 - 273.15)^2]\}^{0.765} N_s L_{s,max}{}^2 Z_8 \times t_f / C_{max}$$

$$\partial f_4/\partial Z_1 = 1.43820 k_b \rho_c k_v [N_s(L_{s,max}Z_8)^3 + m_{3,N,max}Z_7]\{k_g R^{2.67}\{Z_3 C_{max} [a_0 + a_1(T_{c,max}Z_1 - 273.15) + a_2(T_{c,max}Z_1 - 273.15)^2]/[1 - a_0 - a_1(T_{c,max}Z_1 - 273.15) - a_2(T_{c,max}Z_1 - 273.15)^2]\}^{0.765}\}^{0.88} t_f k_b R^{2.67}\{-[a_1 T_{c,max} + 2a_2(T_{c,max}Z_1 - 273.15)T_{c,max}]/[1 - a_0 - a_1(T_{c,max}Z_1 - 273.15) - a_2(T_{c,max}Z_1 - 273.15)^2] + [a_0 + a_1(T_{c,max}Z_1 - 273.15) + - a_2(T_{c,max}Z_1 - 273.15)^2]\{-[a_1 T_{c,max} + 2a_2(T_{c,max}Z_1 - 273.15)T_{c,max}]/\{[1 - a_0 - a_1(T_{c,max}Z_1 - 273.15) - a_2(T_{c,max}Z_1 - 273.15)^2]^2\}\}/\{m_{0,N,max}\{Z_3 C_{max} - [a_0 + a_1(T_{c,max}Z_1 - 273.15) + a_2(T_{c,max}Z_1 - 273.15)^2]/[1 - a_0 - a_1(T_{c,max}Z_1 - 273.15) - a_2(T_{c,max}Z_1 - 273.15)^2]\}^{0.235}\}$$

$$\partial f_4/\partial Z_2 = 0;$$

$$\partial f_4/\partial Z_3 = 1.43820 k_b \rho_c k_v [N_s(L_{s,max}Z_8)^3 + m_{3,N,max}Z_7]\{k_g R^{2.67}\{Z_3 C_{max} [a_0 + a_1(T_{c,max}Z_1 - 273.15) + a_2(T_{c,max}Z_1 - 273.15)^2]/[1 - a_0 - a_1(T_{c,max}Z_1 - 273.15) - a_2(T_{c,max}Z_1 - 273.15)^2]\}^{0.765}\}^{0.88} t_f k_g R^{2.67} C_{max}/\{m_{0,N,max}\{Z_3 C_{max} - [a_0 + a_1(T_{c,max}Z_1 - 273.15) + a_2(T_{c,max}Z_1 - 273.15)^2]/[1 - a_0 - a_1(T_{c,max}Z_1 - 273.15) - a_2(T_{c,max}Z_1 - 273.15)^2]\}^{0.235}\}$$

$$\partial f_4/\partial Z_4 = 0;\ \partial f_4/\partial Z_5 = 0;\ \partial f_4/\partial Z_6 = 0;$$

$$\partial f_4/\partial Z_7 = k_b \rho_c k_v\, m_{3,N,max}\{k_g R^{2.67}\{Z_3 C_{max} - [a_0 + a_1(T_{c,max}Z_1 - 273.15) + a_2(T_{c,max}Z_1 - 273.15)^2]/[1 - a_0 - a_1(T_{c,max}Z_1 - 273.15) - a_2(T_{c,max}Z_1 - 273.15)^2]\}^{0.765}\}^{1.88} t_f / m_{0,N,max}$$

$$\partial f_4/\partial Z_8 = 3\, k_b \rho_c k_v N_s L_{s,max}{}^3 Z_8{}^2 (k_g R^{2.67}\{Z_3 C_{max} - [a_0 + a_1(T_{c,max}Z_1 - 273.15) + a_2(T_{c,max}Z_1 - 273.15)^2]/[1 - a_0 - a_1(T_{c,max}Z_1 - 273.15) - a_2(T_{c,max}Z_1 - 273.15)^2]\}^{0.765}\}^{1.88} t_f / m_{0,N,max}$$

$$\partial f_5/\partial Z_1 = 0.765 m_{0,N,max} Z_4 k_g R^{2.67} t_f\{-[a_1 T_{c,max} + 2a_2(T_{c,max}Z_1 - 273.15)T_{c,max}]/[1 - a_0 - a_1(T_{c,max}Z_1 - 273.15) - a_2(T_{c,max}Z_1 - 273.15)^2] + [a_0 + a_1(T_{c,max}Z_1 - 273.15) - a_2(T_{c,max}Z_1 + 273.15)^2]^*[-a_1 T_{c,max} - 2a_2(T_{c,max}Z_1 - 273.15)T_{c,max}]/[1 - a_0 - a_1(T_{c,max}Z_1 - 273.15) - a_2(T_{c,max}Z_1 - 273.15)^2]/\{\{Z_3 C_{max} - [a_0 + a_1(T_{c,max}Z_1 - 273.15) + a_2(T_{c,max}Z_1 - 273.15)^2]/[1 - a_0 - a_1(T_{c,max}Z_1 - 273.15) - a_2(T_{c,max}Z_1 - 273.15)^2]\}^{0.765}\}^{0.235} m_{1,N,max}\}$$

$$\partial f_5/\partial Z_2 = 0;$$

$$\partial f_5/\partial Z_3 = 0.765\, m_{0,N,max} Z_4\, k_g R^{2.67} t_f\, C_{max}/\{\{Z_3 C_{max} - [a_0 + a_1(T_{c,max}Z_1 - 273.15) + a_2(T_{c,max}Z_1 - 273.15)^2]/[1 - a_0 - a_1(T_{c,max}Z_1 - 273.15) - a_2(T_{c,max}Z_1 - 273.15)^2]\}^{0.235} m_{1,N,max}\}$$

$$\partial f_5/\partial Z_4 = m_{0,\mathrm{N,max}}\, k_g R^{2.67} \{Z_3 C_{\max} - [a_0 + a_1(T_{c,\max}Z_1 - 273.15) + a_2(T_{c,\max}Z_1 - 273.15)^2] / [1 - a_0 - a_1(T_{c,\max}Z_1 - 273.15) - a_2(T_{c,\max}Z_1 - 273.15)^2]\}^{0.765} t_f / m_{1,\mathrm{N,max}}$$

$$\partial f_5/\partial Z_5 = 0;\ \partial f_5/\partial Z_6 = 0;\ \partial f_5/\partial Z_7 = 0;\ \partial f_5/\partial Z_8 = 0;$$

$$\partial f_6/\partial Z_1 = 1.530\, m_{1,\mathrm{N,max}} Z_5\, k_g R^{2.67} t_f \{-[a_1 T_{c,\max} + 2a_2(T_{c,\max}Z_1 - 273.15)T_{c,\max}][1 - a_0 - a_1(T_{c,\max}Z_1 - 273.15) - a_2(T_{c,\max}Z_1 - 273.15)^2] + [a_0 + a_1(T_{c,\max}Z_1 - 273.15) + a_2(T_{c,\max}Z_1 - 273.15)^2][-a_1 T_{c,\max} - 2a_2(T_{c,\max}Z_1 - 273.15)T_{c,\max}] / \{[1 - a_0 - a_1(T_{c,\max}Z_1 - 273.15) - a_2(T_{c,\max}Z_1 - 273.15)^2]^2\}\} / \{\{Z_3 C_{\max} - [a_0 + a_1(T_{c,\max}Z_1 - 273.15) + a_2(T_{c,\max}Z_1 - 273.15)^2] / [1 - a_0 - a_1(T_{c,\max}Z_1 - 273.15) - a_2(T_{c,\max}Z_1 - 273.15)^2]\}^{0.235} m_{2,\mathrm{N,max}}\};$$

$$\partial f_6/\partial Z_2 = 0;$$

$$\partial f_6/\partial Z_3 = 1.530\, m_{1,\mathrm{N,max}} Z_5\, k_g R^{2.67} t_f\, C_{\max} / \{\{Z_3 C_{\max} - [a_0 + a_1(T_{c,\max}Z_1 - 273.15) + a_2(T_{c,\max}Z_1 - 273.15)^2] / [1 - a_0 - a_1(T_{c,\max}Z_1 - 273.15) - a_2(T_{c,\max}Z_1 - 273.15)^2]\}^{0.235} m_{2,\mathrm{N,max}}\};$$

$$\partial f_6/\partial Z_4 = 0;$$

$$\partial f_6/\partial Z_5 = 2\, m_{1,\mathrm{N,max}} k_g R^{2.67} \{Z_3 C_{\max} - [a_0 + a_1(T_{c,\max}Z_1 - 273.15) + a_2(T_{c,\max}Z_1 - 273.15)^2] / [1 - a_0 - a_1(T_{c,\max}Z_1 - 273.15) - a_2(T_{c,\max}Z_1 - 273.15)^2]\}^{0.765} t_f / m_{2,\mathrm{N,max}};$$

$$\partial f_6/\partial Z_6 = 0;\ \partial f_6/\partial Z_7 = 0;\ \partial f_6/\partial Z_8 = 0;$$

$$\partial f_7/\partial Z_1 = 2.295 m_{2,\mathrm{N,max}} Z_6\, k_g R^{267} t_f \{-[a_1 T_{c,\max} + 2a_2(T_{c,\max}Z_1 - 273.15)T_{c,\max}] / [1 - a_0 - a_1(T_{c,\max}Z_1 - 273.15) - a_2(T_{c,\max}Z_1 - 273.15)^2] + [a_0 + a_1(T_{c,\max}Z_1 - 273.15) + a_2(T_{c,\max}Z_1 - 273.15)^2][-a_1 T_{c,\max} - 2a_2(T_{c,\max}Z_1 - 273.15)T_{c,\max}] / \{[1 - a_0 - a_1(T_{c,\max}Z_1 - 273.15) - a_2(T_{c,\max}Z_1 - 273.15)^2]^2 / \{\{Z_3 C_{\max} - [a_0 + a_1(T_{c,\max}Z_1 - 273.15) + a_2(T_{c,\max}Z_1 - 273.15)^2] / [1 - a_0 - a_1(T_{c,\max}Z_1 - 273.15) - a_2(T_{c,\max}Z_1 - 273.15)^2]\}^{0.235} m_{3,\mathrm{N,max}}\};$$

$$\partial f_7/\partial Z_2 = 0;$$

$$\partial f_7/\partial Z_3 = 2.295 m_{2,\mathrm{N,max}} Z_6\, k_g R^{267} t_f\, C_{\max} / \{\{Z_3 C_{\max} - [a_0 + a_1(T_{c,\max}Z_1 - 273.15) + a_2(T_{c,\max}Z_1 - 273.15)^2] / [1 - a_0 - a_1(T_{c,\max}Z_1 - 273.15) - a_2(T_{c,\max}Z_1 - 273.15)^2]\}^{0.235} m_{3,\mathrm{N,max}}\};$$

$$\partial f_7/\partial Z_4 = 0;\ \partial f_7/\partial Z_5 = 0;$$

$$\partial f_7/\partial Z_6 = 3\, m_{2,\mathrm{N,max}}\, k_g R^{267} \{Z_3 C_{\max} - [a_0 + a_1(T_{c,\max}Z_1 - 273.15) + a_2(T_{c,\max}Z_1 - 273.15)^2] / [1 - a_0 - a_1(T_{c,\max}Z_1 - 273.15) - a_2(T_{c,\max}Z_1 - 273.15)^2]^{0.765} t_f / m_{3,\mathrm{N,max}}\};$$

$$\partial f_7/\partial Z_7 = 0;\ \partial f_7/\partial Z_8 = 0;$$

$$\partial f_8/\partial Z_1 = 0.765 k_g R^{2.76}\, t_f \{-[a_1 T_{c,\max} + 2a_2(T_{c,\max}Z_1 - 273.15)T_{c,\max}][1 - a_0 - a_1(T_{c,\max}Z_1 - 273.15) - a_2(T_{c,\max}Z_1$$

$$- 273.15)^2]\} + [a_0 + a_1(T_{c,max}Z_1 - 273.15) + a_2(T_{c,max}Z_1 - 273.15)^2] [- a_1T_{c,max} - 2a_2(T_{c,max}Z_1 - 273.15)T_{c,max}] / \{[1 - a_0 - a_1(T_{c,max}Z_1 - 273.15) - a_2(T_{c,max}Z_1 - 273.15)^2]^2\} / \{\{Z_3C_{max} - [a_0 + a_1(T_{c,max}Z_1 - 273.15) + a_2(T_{c,max}Z_1 - 273.15)^2] / [1 - a_0 - a_1(T_{c,max}Z_1 - 273.15) - a_2(T_{c,max}Z_1 - 273.15)^2]\}^{0.235} L_{s,max}\};$$

$$\partial f_8 / \partial Z_2 = 0;$$

$$\partial f_8 / \partial Z_3 = 0.765k_gR^{2.76} t_f C_{max} / \{\{Z_3C_{max} - [a_0 + a_1(T_{c,max}Z_1 - 273.15) + a_2(T_{c,max}Z_1 - 273.15)^2] / [1 - a_0 - a_1(T_{c,max}Z_1 - 273.15) - a_2(T_{c,max}Z_1 - 273.15)^2]\}^{0.235} L_{s,max}\}$$

$$\partial f_8 / \partial Z_4 = 0;\ \partial f_8 / \partial Z_5 = 0;\ \partial f_8 / \partial Z_6 = 0;\ \partial f_8 / \partial Z_7 = 0;\ \partial f_8 / \partial Z_8 = 0.$$

NOMENCLATURE

A	heat transfer area (m^2)
a_0, a_1, a_2	constants
B	nucleation rate (no. / kg solvent·s)
C	solute concentration (kg solute / kg solvent)
C^*	saturation solute concentration (kg solute / kg solvent)
c_p	specific heat (kJ/ °C·kg crystal)
ΔC	supersaturation (kg solute / kg solvent)
F	Jacobian matrix of $f(x)$; volumetric flow rate of cooling medium (m^3/s)
$f(x)$	nonlinear functions
G	growth rate (m/s)
H	Jacobian matrix of $h(x)$
$h(x)$	linear functions
ΔH	heat of crystals (J/kg crystal)
I	Identity matrix
K	Kalman gain matrix
k_b	nucleation rate coefficient, [(no./kg solute·s)(s/m)$^{1.88}$]
k_c	proportional gain
k_g	growth rate coefficient, [(m/s)(kg solvent/kg solute)$^{0.765}$(s/rev)$^{2.76}$]
k_v	volumetric shape factor of crystals
L	crystal size (m)
M_T	magma density (kg solute / kg solvent)
m_j	jth moment of crystal size distribution (j = 1,2,3,. . .)
N_s	number of seed crystals per unit weight of solvent (no. / kg solvent)
P	state error covariance matrix
Q	covariance matrix of process error
R	covariance matrix of measurement error; stirrer rotational speed (rev/s)

T	temperature (K)
T_j	inside mean cooling jacket temperature (K)
$T_{j,in}$	inlet cooling jacket temperature (K)
t	time (seconds)
t_f	batch time (seconds)
U	overall heat transfer coefficient, W / K (m^2)
V	volume (m^3)
v	measurement error
W	solvent capacity of the crystallizer, kg
W_s	initial weight of the seed crystals, kg
w	process noise
x	state vector
Z	measurements; dimensionless state vector

Greek Symbols

Δ	difference
θ	dimensionless time
ρ	density, kg/m^3
∂	difference

Subscripts

c	crystal; crystallizer
j	jth moment, cooling jacket
k	sampling instant
max	maximum value
N	newly generated crystals
s	seed crystals; solution
T	Total number
w	cooling water
0	initial condition

Superscripts

T	transpose of a vector
*	saturation condition
^	estimate
•	time derivative

MARCEL DEKKER, INC.
270 Madison Avenue, New York, New York 10016

ACKNOWLEDGMENT

The financial support of the Natural Science and Engineering Research Council of Canada is gratefully acknowledged.

REFERENCES

1. Kalman, R.E. A New Approach to Linear Filtering and Prediction Problems. Trans. ASME J. Basic Eng. **1960,** *82* (D), 35.
2. Kalman, R E.; Bucy, R.S. New Results in Linear Filtering and Prediction Theory. Trans. ASME J. Basic Eng. **1961,** *83* (D), 95.
3. Gavalas, G.R.; Seinfeld, J.H. Sequential Estimation of States and Kinetic Parameters in Tubular Reactors with Catalyst Decay. Chem. Eng. Sci. **1969,** *24* (4), 625.
4. Seinfeld, J.H. Optimal Stochastic Control of Nonlinear Systems. AIChE J. **1970,** *16* (4), 1016.
5. Wells, C.H. Application of Modern Estimation Methods and Identification Techniques to Chemical Process. AIChE J. **1971,** *17* (4), 966.
6. Wismer, D.A.; Wells, C.H. A Modern Approach to Industrial Process Control. Automatica **1972,** *8* (2), 117.
7. Coggan, G.C.; Wilson, J.A. On-line State Estimation with a Small Computer. Computer J. **1971,** *14* (7), 61.
8. Hamilton, J.C.; Seborg, D.E.; Fisher, D.G. A Experiment Evaluation of Kalman Filtering. AIChE J. **1973,** *19* (5), 901.
9. Jang, S.S.; Joseph, B.; Muka, H. Comparison of Two Approaches to On-line Parameter and State Estimation of Nonlinear Systems. Ind. Eng. Chem. Processes Des. Dev. **1986,** *25* (3), 809.
10. Stephanopoulos, G.; San, K.Y. Studies on On-line Bioreactor Identification. I. Theory. Biotechnol. Bioeng. **1984,** *26* (10), 1176.
11. San, K.Y.; Stephanopoulos, G. Studies on On-line Bioreactor Identification. II. Numerical and Experimental Results. Biotechnol. Bioeng. **1984,** *26* (10), 1176.
12. Ramirez, W.F. Optimal State and Parameter Identification. An Application to Batch Fermentation. Chem. Eng. Sci. **1987,** *42* (11), 2749.
13. Dimitratos, J.; Georgakis, C.; El-Aasser, M.S.; Klein, A. Dynamic Modeling and State Estimation for an Emulsion Copolymerization Reactor. Computers Chem. Eng. **1989,** *13* (1/2), 21.
14. Kozub, D.J.; Macgregor, J.F. State Estimation for Semi-Batch Polymerization Reactors. Chem. Eng. Sci. **1992,** *47* (5), 1047.
15. Myers, M.A.; Luecke, R.H. Process Control Applications of an Extended Kalman Filter Algorithm. Computers Chem. Eng. **1991,** *15* (12), 853.

MARCEL DEKKER, INC.
270 Madison Avenue, New York, New York 10016

16. Lee, J.H.; Ricker, N.L. Extended Kalman Filter Based Nonlinear Model Predictive Control. Ind. Eng. Chem. Res. **1994,** *33* (6), 1530.
17. Ahn, S.M.; Park, M.J.; Rhee, H.K. Extended Kalman Filter Based Nonlinear Model Predictive Control for a Continuous MMA Polymerization Reactor. Ind. Eng. Chem. Res. **1999,** *38* (10), 3942.
18. Jazwinski, A.H. *Stochastic Processes and Filtering Theory;* Academic Press: New York, 1970.
19. Gelb, A., Ed. *Applied Optimal Estimation*; The M.I.T. Press: Cambridge, Mass, 1974; 180–228.
20. Xie, W.; Rohani, S.; Phoenix, A. Dynamic Modeling and Operation of a Seed Batch Cooling Crystallizer. Chem. Eng. Commun. **2001,** in press.
21. Tavare, N.S.; Garside, J. Simultaneous Estimation of Crystal Nucleation and Growth Kinetics from Batch Experiments. Chem. Eng. Res. Des. **1986,** *64* (2), 109.
22. Redman, T.P.; Rohani, S. On-line Measurement of Supersaturation of a KCl-NaCl Aqueous Solution Based on Density Measurement. Can. J. Chem. Eng. **1994,** *72* (1), 64–71.
23. Mullin, J.W. *Crystallization*, 3rd Ed.; Butterworth Heinemann Ltd: Oxford, UK, 1993.
24. Manjaly, J.M. Ph.D. diss. Crystallization Kinetics of Potash Alum., University of London, 1978.

Received August 2000

MARCEL DEKKER, INC.
270 Madison Avenue, New York, New York 10016